Biosensors and Bioelectronics 38 (2012) 239–244

Contents lists available at SciVerse ScienceDirect

Biosensors and Bioelectronics

journal homepage: www.elsevier.com/locate/bios

MgFe-layered double hydroxide modified electrodes for direct electron transfer of heme proteins

Maoguo Li *, Huiqin Ji, Yinling Wang *, Lin Liu, Feng Gao

Key Laboratory of Chemo-Biosensing, Anhui Province, College of Chemistry and Materials Science, Anhui Normal University, Wuhu 241000, PR China

ARTICLE INFO

Article history:
Received 15 March 2012
Received in revised form
25 May 2012
Accepted 28 May 2012
Available online 6 June 2012

Keywords:
Layered double hydroxides
Heme proteins
Direct electron transfer
Hydrogen peroxide
Biosensors

ABSTRACT

In this study, the Fe-based layered double hydroxides (Mg_3Fe LDH) were used to immobilize heme proteins including hemoglobin (Hb), myoglobin (Mb) and horseradish peroxidase (HRP) for fabrication of heme/Mg_3Fe LDH film on glassy carbon electrode (Mg_3Fe-heme/GCE). The possible role of iron in framework of LDH to promote direct electron transfer (DET) of heme proteins was investigated using an LDH containing non-iron as a reference. Hb was selected as a model protein for studying the electrocatalytic activity of immobilized heme in LDH film. The Mg_3Fe-Hb/GCE displayed an enhanced electrocatalytic reduction towards H_2O_2. The biosensor showed a very low detection limit (0.036 μM) and apparent Michaelis–Menten constant (7.98 μM). This work outlines that Fe-based LDH modified electrode provides a promising platform for immobilization of heme proteins and development of sensitive biosensors.

1. Introduction

Biosensors based on the direct electron transfer (DET) between redox proteins and electrode surface have received considerable attentions since the reversible electrochemistry of cytochrome *c* realized on modified electrodes in 1977 (Eddowes and Hill, 1977; Yeh and Kuwana, 1997), because they can be used without the addition of mediators or promoters onto the electrode surface or into the solution. In addition to clinical diagnosis (D'Orazio, 2011), such sensors offer great promise for other important applications, ranging from bioprocess monitoring to food analysis (Nöll and Nöll, 2011). For applications in biosensors, the proteins should be immobilized on the electrode surface to avoid many complications linked to the solution system. Recently, various nanostructures, such as metal, metal oxide, conducting polymer and carbon materials, have been extensively used for fabrication of biosensors, as illustrated by the several review articles (Feigel et al., 2011; Liu, 2008; Deepshikha and Basu, 2011; Cosnier and Holzinger, 2011; Kuila et al., 2011). Recently, inorganic nanoparticles have become more attractive due to their desirable properties, such as good biocompatibility, high chemical and physical stability, and low production costs.

Clays are a typical class of two-dimensional layered inorganic materials, with variable chemical composition and unique structure. Clay can be divided into two main classes: cationic clays and anionic clays, also known as layered double hydroxides (LDH). Following in the footsteps of DET for cytochrome *c* at clay-modified electrode (Lei et al., 1999), various clay-modified electrodes have designed as powerful tools to immobilize heme proteins, and have resulted in high-performance biosensors based on the DET of those proteins (Mousty, 2004, 2010). In particular, very recently, increasing attention has been paid to the immobilization of heme proteins in LDH matrices, due to that LDH could immobilize enzyme on the electrode surface more efficiently and give better analytical characteristics than the cationic clays in all cases (de Melo et al., 2002; Shan et al., 2003; Cosnier et al., 2006). Our group has studied the electrochemical and electrocatalytic properties of hemoglobin (Hb) in ZnAl-SDS LDH film modified electrode (Li et al., 2008). Subsequently, the DET of horseradish peroxidase (HRP) and Hb were achieved directly at NiAl-NO_3 LDH (Chen et al., 2008) and MgAl-Cl LDH (Charradi et al., 2010), whereas the adsorption of myoglobin (Mb) was investigated onto NiAl-Br LDH colloid suspension (Bellezza et al., 2009). All these studies showed that LDH could provide a suitable microenvironment to immobilize heme proteins and facilitate the DET between the electroactive heme sites of the proteins and the underlying electrodes. Furthermore, the proteins in LDH films generally retained their native structure without modification of their heme Fe(III)/(II) electroactive group.

It has been demonstrated that the presence of trace iron in the crystal structure of natural smectite clays influences their physical and chemical properties greatly. For instance, Charradi et al. (2009) have shown that nontronite, one kind of cationic clay containing high amount of structural iron (in the octahedral

* Corresponding authors. Tel.: +86 553 386 9302; fax: +86 553 386 9303.
E-mail addresses: limaoguo@mail.ahnu.edu.cn, limaoguo@yahoo.com.cn (M. Li), wyinl@mail.ustc.edu.cn (Y. Wang).

0956-5663/$ - see front matter © 2012 Elsevier B.V. All rights reserved.
http://dx.doi.org/10.1016/j.bios.2012.05.035

sheet, 4.2 mmol g^{-1}), enhanced significantly DET of Hb. No redox peak was observed at the electrode coated with Hb immobilized in synthetic montmorillonite containing non-iron impurities (MS) or synthetic saponite (SapSF), which has Fe(III) only in the tetrahedral sheet. In contrast, a reversible signal with low peak current intensity was also observed at synthetic montmorillonite presenting Fe(III) (0.41 mmol g^{-1}) only in the octahedral sheet (MSF). Since LDH could give best analytical characteristics in all cases related to enzyme immobilization (Mousty, 2010), LDH containing iron in the framework may be more suitable to immobilize heme proteins and realize the DET. However, to the best of our knowledge, to date there has been no report on the DET of heme proteins in Fe-based LDH.

In this present work, we report the use of MgFe-Cl LDH as the matrix for immobilization of Hb, Mb and HRP. The DET of these heme proteins was realized easily at the Fe-based LDH modified electrode as expected. We anticipated that the Fe (III) in the framework of LDH might play a certain role in the direct electrochemistry of heme proteins. Hb was selected as a model protein for studying the electrochemical and electrocatalytic behavior of the proteins entrapped Fe-based LDH modified electrode. Our results indicate that the low-cost synthetic LDH containing Fe(III) modified electrode may provide a promising platform for the development of biosensors.

2. Materials and methods

2.1. Reagents and chemicals

Hemoglobin (Hb) (from bovine blood) was purchased from Tokyo Kasei Kogyo Co., Ltd. (Japan). Horseradish peroxidase (HRP) and myoglobin (Mb) were purchased from Sangon Biotech Co., Ltd (China). Other chemicals were obtained from Chemical Reagent Company of Shanghai (China). All the solutions were prepared with Milli-Q purified water (Millipore, ≥ 18.2 M Ω cm) and decarbonated water, purged with highly purified nitrogen before experiments.

2.2. Apparatus

All electrochemical experiments were performed in a conventional three-electrode cell controlled by a CHI660C electrochemical workstation (CH Instruments, Shanghai, China). A three-electrode system was employed with a platinum wire (ref CHI115) as the counter electrode, a saturated calomel electrode (SCE, ref CHI150) as the reference electrode, and a modified (or bare) glassy carbon electrode (GCE, ref CHI104) as the working electrode. All electrochemical experiments were performed at room temperature. Powder X-ray diffraction (XRD) data were recorded by a Shimadzu XRD−6000 X-ray diffractometer (Shimadzu, Japan) based on Cu Kα radiation (λ=0.15406 nm). The 2θ angle of the diffractometer was gradated from 5° to 70° at a scan rate of 0.02° s^{-1}. The morphologies of LDH were examined with a Hitachi S-4800 scanning electron microscope (SEM, Hitachi, Japan). Fourier transform infrared (FT-IR) spectra were taken on a FTIR-8400S Fourier transform infrared spectrophotometer after 20 scans within 4000–400 cm^{-1} at a resolution of 8 cm^{-1} by measuring the IR absorbance of a KBr disk containing of 1–2 wt% of the sample. UV-visible (UV–vis) absorption spectroscopy measurement was carried out with a U-2450 (Shimadzu, Japan). The metal contents of the Mg-Al-HCF LDH samples were determined by inductively coupled plasma optical emission spectrophotometry (ICP-OES) on a Perkin Elmer Optima 5300DV after a weighed amount of sample was dissolved in a dilute HCl solution.

2.3. The synthesis of MgFe LDH

The MgFe-Cl LDH was synthesized by the coprecipitation method according to the reference with a slight modification (Constantino and Pinnavaia, 1995; Aisawa et al., 2007). In a typical procedure, a mixed salt solution containing Mg^{2+} and Fe^{3+} was prepared by weighted $MgCl_2 \cdot 6H_2O$ and $FeCl_3 \cdot 6H_2O$. The total Mg^{2+} and Fe^{3+} concentrations sustained 1 M with Mg/Fe molar ratios of 2:1, 3:1 and 4:1. Then, the solution pH was adjusted at 10.0 by dropwise addition of 1 M NaOH solution under vigorous stirring. The slurry was aged at 100 °C for 4 h in an oil-bath. The resulting solid product was filtered, washed with water and anhydrous ethanol for several times, and finally dried at 70 °C over night in a decompression oven. Mg_3Al LDH (Mg/Al molar ratio of 3:1), used as a reference, was also synthesized according to the aforementioned method.

2.4. Preparation of protein-LDH hybrids on GCE

The different colloidal suspension (2 mg mL^{-1}) was prepared by dispersing desired LDH in water with stirring for approximately 24 h. Heme was dissolved in water with a concentration of 10 mg mL^{-1}. 10 μL of the aqueous mixtures containing a 1:1 (or other mass ratios) heme/LDH was spread on the surface of the pretreated GCE and then dried in a fridge overnight. Before use, the modified electrode was exposed in saturated glutaraldehyde vapor for 10 min for cross-linking of the entrapped proteins. Finally, LDH gel formation was achieved and glutaraldehyde traces were removed by incubation of the modified electrode in 0.1 M pH 7.0 phosphate buffer solutions (PBS) for 25 min.

3. Results and discussion

3.1. The characterization of MgFe-Cl LDH

The XRD patterns of MgAl-Cl LDH (curve a in Fig. 1A) and MgFe-Cl LDH with different Mg/Fe molar ratios (curves b–d) showed intense basal reflection series (00*l*), indicative of the well crystalline nature of them. The 003 reflections were all located on almost the 2θ angle of ~10.9°, indicating a basal interlayer spacing of ~0.78 nm for Cl-LDH, quite similar to those reported elsewhere (Constantino and Pinnavaia, 1995; Liu et al., 2006, 2007). Compared to MgAl-Cl LDH, the peaks were broader and lower for all MgFe-Cl LDH, which indicated that MgFe-Cl LDH was less crystalline than the MgAl-Cl LDH prepared under the same condition.

Fig. 1B presents an SEM image of a typical LDH sample with Mg/Fe molar ratio of 3:1. The morphology of the LDH was observed clearly via SEM. The SEM investigation shows that the LDH prepared by the precipitation method is nano-scaled and three-dimensional with a size of 40–60 nm. The FT-IR spectra of the MgAl-Cl LDH and MgFe-Cl LDH (Mg/Fe molar ratio equals to 3) are shown in supplementary information (Fig. S1). They are typical of Cl-LDH materials, as featured both for MgAl and MgFe LDH by a broad band at 3420 cm^{-1} (ν_{OH}), a peak at 1630 cm^{-1} (δH_2O), a peak at 1355 cm^{-1} ($\nu_{CO_3^{2-}}$) (due to CO_3^{2-} converted from CO_2 captured from air during reacting and washing), and bands at 783, 625, and 430 cm^{-1} (due to M–O vibrations and M–O–H bending) (Nakamoto, 1997).

3.2. The electrochemical behavior of heme in LDH film modified GCE

The electrochemical properties of several heme proteins (Hb, Mb and HRP) LDH modified electrodes were studied by cyclic voltammetry (CV) in a 0.1 M pH 7.0 PBS. It should be noted that

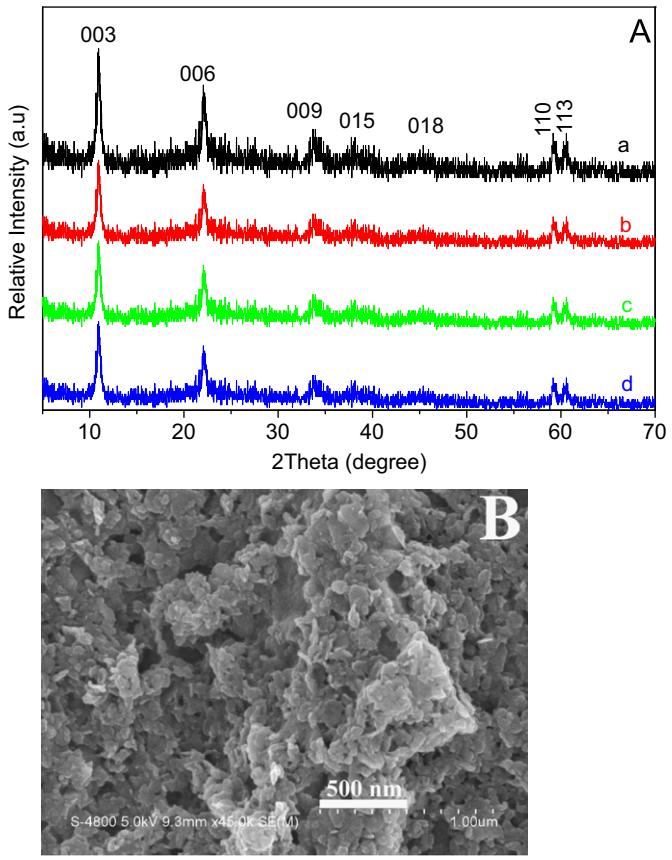

Fig. 1. (A) XRD patterns of (a) MgAl-Cl LDH and (b–d) MgFe-Cl LDH with Mg/Fe mole ratios of 2:1, 3:1 and 4:1. (B) Selected SEM image of MgFe-Cl LDH with Mg/Fe mole ratio of 3:1.

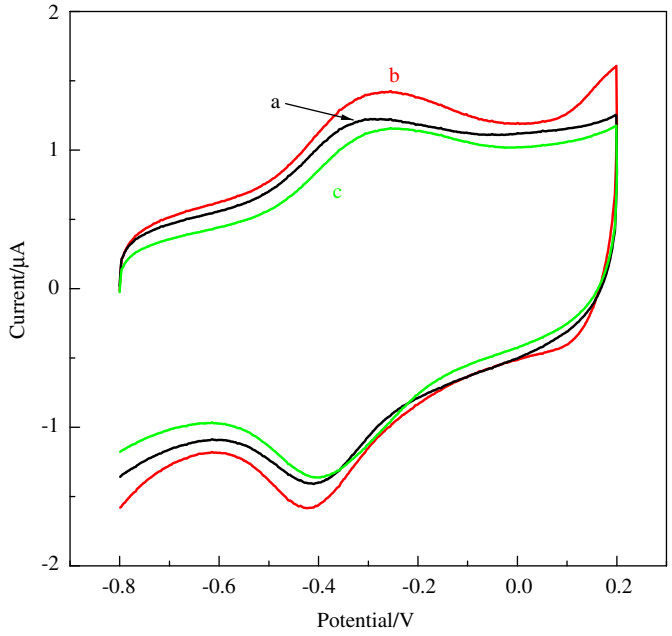

Fig. 2. Cyclic voltammograms of Mg_xFe-Hb/GCE in 0.1 M pH 7.0 PBS at 200 mV s^{-1}. The *x* is (a) 2, (b) 3, and (c) 4, respectively.

Hb immobilized into MgFe-Cl LDH with Mg/Fe molar ratio of 3:1 gave significantly higher electrochemical signals than MgFe-Cl LDH with other Mg/Fe molar ratios under the same conditions (Fig. 2). The high positive charges of Mg_2Fe LDH and the low Fe(III) contents of Mg_4Fe LDH led to a decreased DET of Hb. Obviously, the Fe-contents and charges of LDH play a very important role in the adsorption site of Hb during the DET between Hb and underlying electrode. Based on the above, Mg/Fe molar ratio of 3:1 is given preference in this work. The heme proteins and Mg_3Fe LDH modified GCE is denoted as Mg_3Fe-Heme/GCE. The Mg_3Al-Hb/GCE, modified with non-iron Mg_3Al LDH, was used as a reference. As shown in Fig. 3, all three kinds of heme proteins displayed the well-defined quasi-reversible cyclic voltammograms with a formal potential ($E^{\circ\prime}$) of −0.358 V, corresponding to the reversible reduction of heme.

$$\text{Heme-Fe(III)} + H^+ + e^- \rightarrow \text{Hb-Fe(II)}$$

However, no peaks were observed for Mg_3Al-Hb/GCE (Fig. S2, trace a) when the ratio Hb/LDH is also 1, quite similar to the previous reports on Mg_2Al-Hb and Zn_2Al-Hb modified electrodes (Charradi et al., 2010; Li et al., 2008). In contrast, as previously reported (Charradi et al., 2010), a small pair of redox peaks can be observed when the ratio Hb/LDH was increased to 5 (Fig. S2, trace b).

Our results indicated that iron atoms in framework of LDH played a very important role in promoting DET of heme proteins. Mousty and coworkers (Charradi et al., 2009) have pointed out that iron atoms can play the role of electron relay in the electron-hopping mechanism enhancing the amount of heme which can be involved into the electron transfer process, as shown in Fig. S3.

At the Mg_3Fe-Hb/GCE, the peak height varies linearly with the scan rate (Fig. 4); this relationship shows that the redox couple is surface-confined. According to the slope of the I_p–ν curve and Laviron's equation (Laviron, 1979), $I_p = n^2F^2\nu A\Gamma/4RT$, the average surface coverage (Γ) of Hb on the surface of modified electrode was 2.29×10^{-10} mol cm^{-2}, which was approximately 12 times of the theoretical monolayer coverage (1.89×10^{-11} mol cm^{-2}) (Muirhead and Perutz, 1963). At the same time, a negative shift in potential for both anodic and cathodic peaks was along with an increase of the solution pH (Fig. S4). The apparent formal peak potential ($E^{\circ\prime}$) had a linear relationship with pH from pH 5.0 to 9.0 with a slope of −57.2 mV/pH. This slope is very close to the theoretical value of −58.6 mV/pH at 298.15 K for a reversible, one-proton coupled with one-electron redox reaction process of Hb.

3.3. The electrocatalytic activity of immobilized heme in LDH film

Hb was selected as a model protein for studying the electrocatalytic activity of immobilized heme in LDH film. The electrocatalytic reduction of H_2O_2 at the Mg_3Fe-Hb/GCE was investigated by CV and amperometry. When 60 μM H_2O_2 was added in PBS, an increase in the reduction peak was observed with the decrease in the oxidation peak (Fig. 5A). The results indicate that LDH provides a favorable microenvironment for immobilization of Hb and the embedded Hb retains the biocatalytic activity, which also testified by UV–vis spectroscopy. The dry Hb-LDH cast on quartz slides showed the same peak position (about 410 nm) as the free Hb dry film (Fig. S5). To further illustrate the relationship between the electrocatalytic reduction current and the concentration of H_2O_2, the steady-state amperometric response of modified electrode to successive additions of H_2O_2 up to 3.75 μM was recorded at a fixed applied potential of −0.35 V (Fig. 5B). The response time to reach 95% of the maximum current was about 5 s, demonstrating a fast electrocatalytic response. The linear response to H_2O_2 ranging from 0.07 to 2.51 μM (R^2=0.9916), with a relative standard deviations (RSD) of 4.6%. The limit of detection was 0.036 μM for a signal-to-noise ratio of 3, which was lower than that on other inorganic matrices, such as 0.6 μM on doped titanium dioxide (Wei et al., 2011), 0.68 μM on

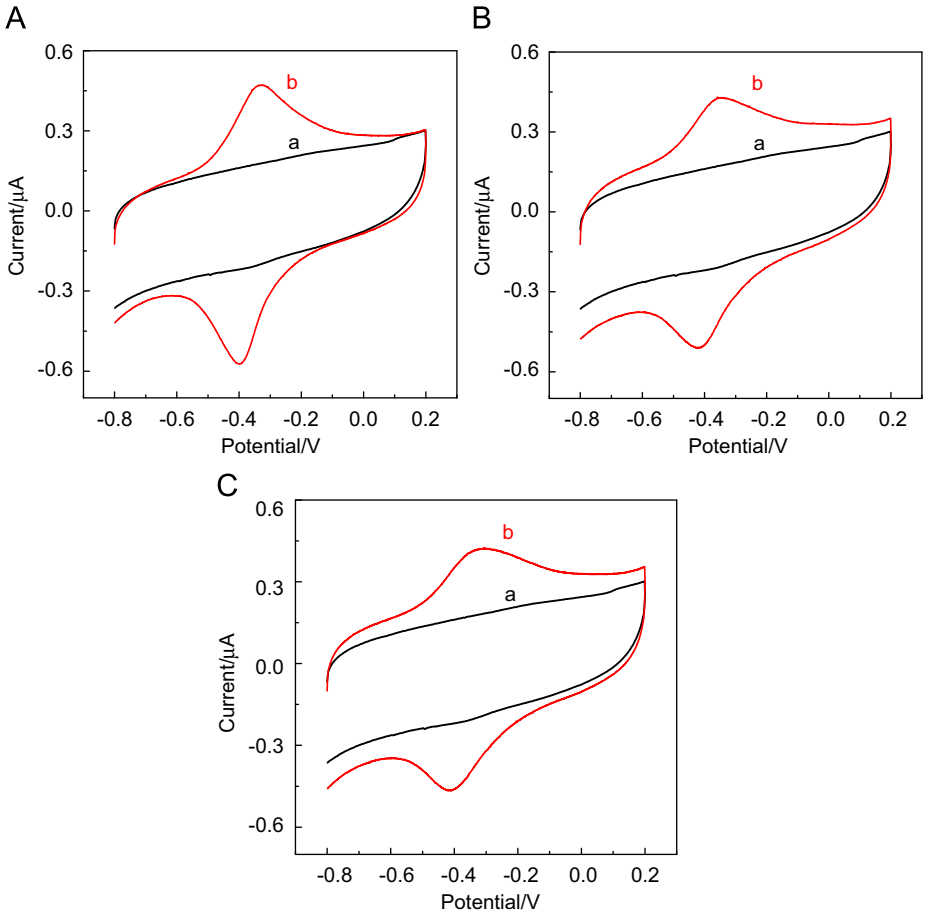

Fig. 3. Cyclic voltalmmograms of (a) Mg_3Fe/GCE and (b) Mg_3Fe-Heme/GCE in 0.1 M pH 7.0 PBS at 100 mV s^{-1}. Heme proteins are (A) Hb, (B) Mb, and (C) HRP, respectively.

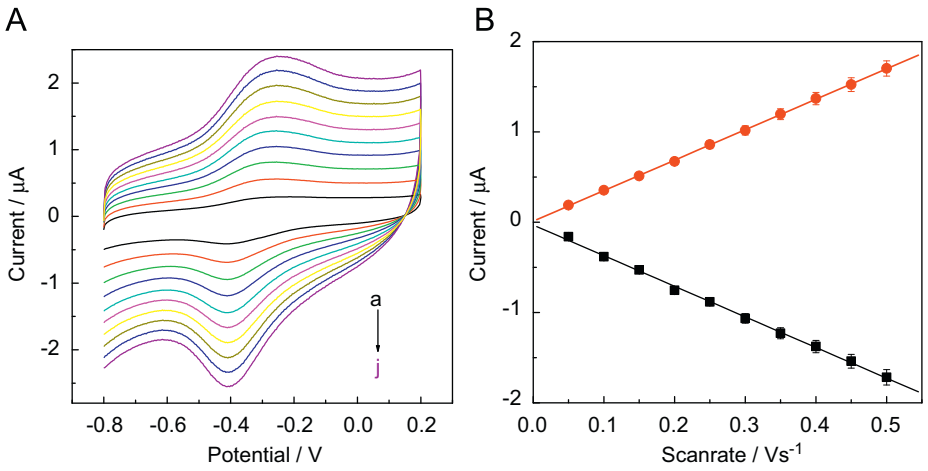

Fig. 4. (A) Cyclic voltalmmograms of Mg_3Al-Hb/GCE in 0.1 M pH 7.0 PBS at different scan rates. The scan rates are (a) 50, (b) 100, (c) 150, (d) 200, (e) 250, (f) 300, (g) 350, (h) 400, (i) 450, and (j) 500 V s^{-1}, respectively. (B) The linear dependence of anodic and cathodic peak currents vs. scan rate.

walnutlike NiO microspheres (Dong et al., 2011), and 0.16 μM on magnetic core-shell Fe_3O_4@Al_2O_3 nanoparticles (Peng et al., 2011). The sensitivity was 27.6 μA mM^{-1}, indicating Hb immobilized in Mg_3Fe LDH film exhibited excellent bioelectrocatalytic activity to H_2O_2 reduction.

It is well known that the apparent Michaelis–Menten constant (K_M^{app}) can provide an indication of the enzyme–substrate kinetics. The K_M^{app} value can be calculated from the electrochemical version of the Lineweaver–Burk equation (Kamin and Wilson, 1980)

$$\frac{1}{I_{ss}} = \frac{K_M^{app}}{I_{max}}\frac{1}{C} + \frac{1}{I_{max}}$$

Here, I_{ss} is the steady state current after the addition of substrate, C is the bulk concentration of the substrate, and I_{max} is the maximum current measured under saturated substrate conditions. A plot of $1/I_{ss}$ vs. $1/C$ will give a straight line with the

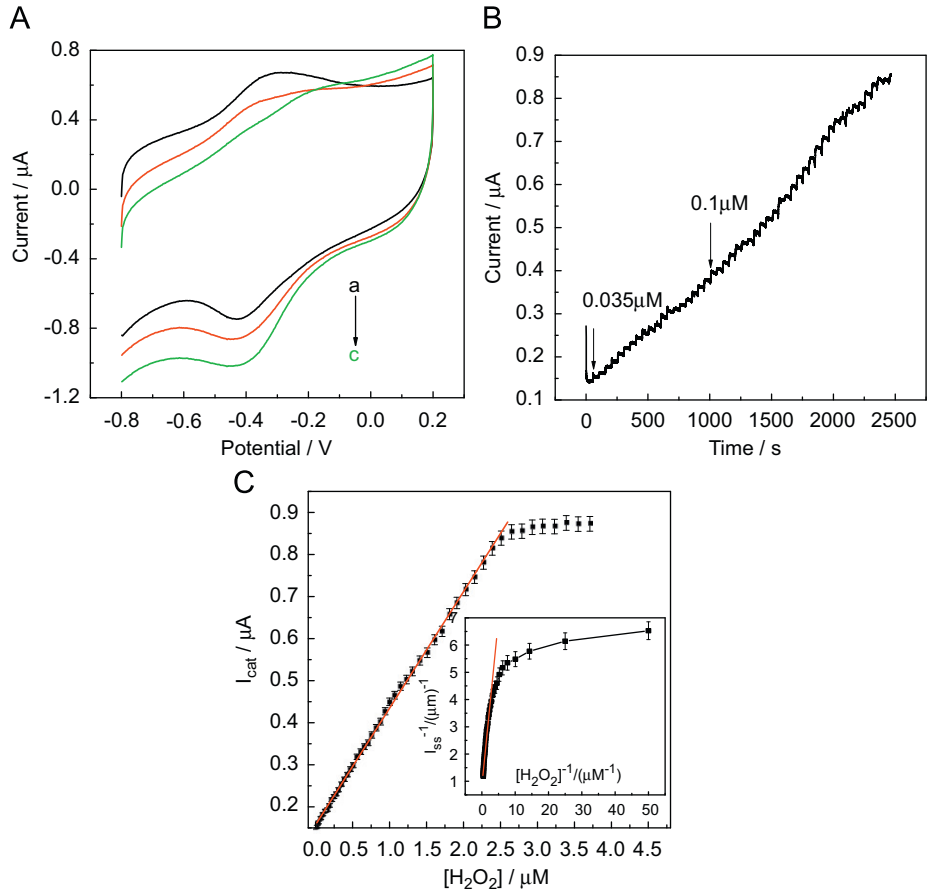

Fig. 5. (A) Cyclic voltammograms of Mg_3Fe-Hb/GCE in 0.1 M pH 7.0 PBS containing (a) 0, (b) 60 and (c) 120 μM H_2O_2. The scan rate is 100 mV s^{-1}; (B) The amperometric response of Mg_3Fe-Hb/GCE at −0.35 V upon successive additions of H_2O_2 0.1 M pH 7.0 PBS; (C) The calibration curve of *i*–*c* obtained by amperometry. Inset: linear calibration curve of I_{ss}^{-1} vs. $[H_2O_2]^{-1}$.

Table 1
Comparison of analytical performance of different biosensors for the determination of H_2O_2.

Biosensor	Linear range (μM)	Detection limit (μM)	Sensitivity (μA mM^{-})	K_M^{app} (μM)	Refs.
HRP@SiO_2/GC electrode	0.002–0.012 0.012–6.7	0.000128	–	0.088	Cao et al. (2012)
Ti/Au/BP/HRP-MB electrode	0.1–500	0.075	54000	–	Chatterjee and Chen (2012)
Hb/3DOM GTD/ITO electrode	5.0–1000	0.6	144.5	–	Wei et al. (2011)
F-NiO/IL/Hb-CP electrode	2.0–1050	0.68	15.7	180	Dong et al. (2011)
Hb/Fe_3O_4@Al_2O_3/MGC electrode	0.51–111.20	0.16	–	120	Peng et al. (2011)
Mg_3Fe-Hb/GC electrode	0.07–2.51	0.036	27.6	7.98	This work

slope equal to K_M^{app}/I_{max} and intercept equal to $1/I_{max}$ (Inset in Fig. 5C). The K_M^{app} for the enzymatic activity of the Mg_3Fe-Hb/GCE to H_2O_2 was estimated to be 7.98 μM. This low value for K_M^{app} implies that the as-prepared modified electrode had a higher affinity for H_2O_2 than our previous reported ZnAl-SDS-Hb/GCE (Li et al., 2008). Compared with other H_2O_2 biosensors listed in Table 1, the biosensor had wider linear range, lower detection limit, higher sensitivity and smaller K_M^{app}.

3.4. The reproducibility and stability of biosensors

Five repetitive measurements by amperometry at five Mg_3Fe-Hb/GCEs which were prepared independently were carried out in 1.0 μM H_2O_2 and a RSD of 3.7% was observed, which indicated that the biosensors displayed an acceptable reproducibility. To estimate the operational stability of the as-prepared biosensor, a continuous measurement of CV was carried out for 60 min in a 50.0 μM H_2O_2 solution. It was found that the peak current for H_2O_2 reduction retained 96.3% of its initial value and no obvious potential shift was observed. The result shows that the modified electrode has good operational stability. The storage stability of the biosensor was monitored for two weeks. It was found that the current response was no apparent decrease in the first continuous five days by everyday use and stored in 0.1 M pH 7.0 PBS at 4 °C. After 14 day, the reduction current of 1.0 μM of H_2O_2 retained 95.7% of its initial value, indicating that the biosensor has good storage stability.

4. Conclusions

Mg_3Fe LDH were synthesized facilely by the coprecipitation method and used for immobilization of heme proteins on GC electrode, followed by glutaraldehyde cross-linking. Our results

show that the Fe-based LDH can enhance DET between heme proteins and the underlying electrode, iron atoms in framework of LDH playing the role of electron relay. Taking advantage of the favorable microenvironment provided by LDH, the Hb cross-linked by glutaraldehyde in the film retains the bioelectrocatalytic activity for the H_2O_2 reduction even at the very low H_2O_2 level. This work outlines that Fe-based LDH modified electrode provides a promising platform for immobilization of heme proteins and development of sensitive biosensors.

Acknowledgments

M. Li and Y. Wang are grateful for the financial support from the Natural Science Foundation of China (Grant nos. 21075001 and 20801001) and the Anhui Provincial Natural Science Foundation (Grant no. 11040606M46). F. Gao would also like to thank the Natural Science Foundation of China (Grant nos. 21055001 and 21175002) for their financial support.

Appendix A. Supplementary Information

Supplementary data associated with this article can be found in the online version at http://dx.doi.org/10.1016/j.bios.2012.05.035.

References

Aisawa, S., Higashiyama, N., Takahashi, S., Hirahara, H., Ikematsu, D., Kondo, H., Nakayama, H., Narita, E., 2007. Applied Clay Science 35, 146–154.
Bellezza, F., Cipiciani, A., Latterini, L., Posati, T., Sassi, P., 2009. Langmuir : the ACS Journal of Surfaces and Colloids 25, 10918–10924.
Cao, X., Yu, J., Zhang, Z., Liu, S., 2012. Biosensors and Bioelectronics 35, 101–107.
Charradi, K., Forano, C., Prevot, V., Ben Haj Amara, A., Mousty, C., 2009. Langmuir : the ACS Journal of Surfaces and Colloids 25, 10376–10383.
Charradi, K., Forano, C., Prevot, V., Madern, D., Ben Haj Amara, A., Mousty, C., 2010. Langmuir : the ACS Journal of Surfaces and Colloids 26, 9997–10004.
Chatterjee, S., Chen, A., 2012. Biosensors and Bioelectronics 35, 302–307.
Chen, X., Fu, C., Wang, Y., Yang, W., Evans, D.G., 2008. Biosensors and Bioelectronics 24, 356–361.
Constantino, V.R.L., Pinnavaia, T.J., 1995. Inorganic Chemistry 34, 883–892.
Cosnier, S., Holzinger, M., 2011. Chemical Society Reviews 40, 2146–2156.
Cosnier, S., Mousty, C., Gondran, C., Lepellec, A., 2006. Materials Science Engineering C 26, 442–447.
Deepshikha, Basu T., 2011. Analytical Letters 44, 1126–1171.
de Melo, J.V., Cosnier, S., Mousty, C., Martelet, C., Renault, N.J., 2002. Analytical Chemistry 74, 4037–4043.
Dong, S., Zhang, P., Liu, H., Li, N., Huang, T., 2011. Biosensors and Bioelectronics 26, 4082–4087.
D'Orazio, P., 2011. Clinica Chimica Acta; International Journal of Clinical Chemistry 412, 1749–1761.
Eddowes, M.J., Hill, H.A.O., 1977. Journal of the Chemical Society, Chemical Communications, 771–772.
Feigel, I.M., Vedala, H., Star, A., 2011. Journal of Materials Chemistry 21, 8940–8954.
Kamin, R.A., Wilson, G.S., 1980. Analytical Chemistry 52, 1198–1205.
Kuila, T., Bose, S., Khanra, P., Mishra, A.K., Kim, N.H., Lee, J.H., 2011. Biosensors and Bioelectronics 26, 4637–4648.
Laviron, E., 1979. Journal of Electroanalytical Chemistry 100, 263–270.
Lei, C., Lisdat, F., Wollenberger, U., Scheller Frieder, W., 1999. Electroanalysis 11, 274–276.
Liu, A., 2008. Biosensors and Bioelectronics 24, 167–177.
Liu, Z., Ma, R., Ebina, Y., Iyi, N., Takada, K., Sasaki, T., 2007. Langmuir : the ACS Journal of Surfaces and Colloids 23, 861–867.
Liu, Z., Ma, R., Osada, M., Iyi, N., Ebina, Y., Takada, K., Sasaki, T., 2006. Journal of the American Chemical Society 128, 4872–4880.
Li, M., Chen, S., Ni, F., Wang, Y., Wang, L., 2008. Electrochimica Acta 53, 7255–7260.
Mousty, C., 2004. Applied Clay Science 27, 159–177.
Mousty, C., 2010. Analytical and Bioanalytical Chemistry 396, 315–325.
Muirhead, H., Perutz, M.F., 1963. Nature 199, 633–638.
Nöll, T., Nöll, G., 2011. Chemical Society Reviews 40, 3564–3576.
Nakamoto, K., 1997. Infrared and Raman Spectra of Inorganic and Coordinate Compounds. Part A. John Wiley and Sons, New York.
Peng, H.P., Liang, R.P., Qiu, J.D., 2011. Biosensors and Bioelectronics 26, 3005–3011.
Shan, D., Cosnier, S., Mousty, C., 2003. Analytical Chemistry 75, 3872–3879.
Wei, N., Xin, X., Du, J., Li, J., 2011. Biosensors and Bioelectronics 26, 3602–3607.
Yeh, P., Kuwana, T., 1997. Chemistry Letters, 1145–1148.